

LINKAGES BETWEEN MULTI-SCALE GLOBAL SEA SURFACE TEMPERATURE CHANGE AND PRECIPITATION VARIABILITIES IN THE U.S.

K.-M. Lau* and Hengyi Weng

Laboratory for Atmospheres, NASA/Goddard Space Flight Center
Greenbelt, Maryland, USA

1. INTRODUCTION

A growing number of evidence indicates that there are coherent patterns of variability in sea surface temperature (SST) anomaly not only at interannual timescale, but also at decadal-to-interdecadal timescale and beyond (Folland et al. 1984; Latif and Barnett 1996; Chang et al. 1997; Zhang et al. 1997; Lau and Weng 1998). The multi-scale variabilities of SST anomaly have shown great impacts on world climate. In this work, we analyze multiple timescales contained in the globally averaged SST anomaly with and their possible relationship with the summer and winter rainfall in the United States over the past four decades.

2. DATA AND METHODS

The SST anomaly is based on $1^\circ \times 1^\circ$ lon \times lat GISST2.3b data set provided by U. S. Meteorological Office, with the climatology for the period of 1961-90. The U.S. rainfall anomaly is based on the 102-division data set provided by the Climate Prediction Center, NOAA. The relationship between the SST anomaly and the rainfall anomaly in the U.S. obtained here is for 1955-1997 summers and 1955/56-1997/98 winters. However, the whole SST record (1871-1997/98) is used in wavelet transform for continuation around 1955. Since there are apparent trends in these seasonal mean SST anomalies, a linear trend has been removed from each time series before wavelet analysis is performed. After separating the time series of the globally averaged SST anomaly into different timescales, the linear trend that is a part of the long-term trend is then added back to the component with centennial variability (CEV, timescales longer than 64 years) as the trend (TRD) for the period of 1955-97. The signals with timescales between 8 years and 64 years are combined as "decadal-to-interdecadal variability" (DIV), and those with timescales less than 8 years are combined as "interannual variability" (IAV). For each season, the linear regression is performed for these three temporal components (IAV, DIV and TRD) with global grid SST anomaly between $40^\circ\text{S} - 60^\circ\text{N}$, and with the rainfall anomaly in the U.S. In the figures presented here, the subscripts "s" and "w" indicate "summer" and "winter", respectively.

*Corresponding author address: Dr. K.-M. Lau, Code 913, NASA/GSFC, Greenbelt, MD 20771, USA. E-Mail: lau@climate.gsfc.nasa.gov

3. GLOBAL MEAN SST ANOMALY

Lau and Weng (1998) analyzed interannual, decadal-to-interdecadal and global warming signals in globally averaged annual mean sea surface temperature for the period of 1955-97 by using NOAA's 10 degree resolution data. Here we study the difference between summers and winters at the timescales of IAV, DIV and TRD. Fig. 1 presents the global wavelet spectra of linearly detrended SST anomaly in JJA and DJF for the period of 1955-97. The main difference between the two seasons is at the IAV timescale. The dominant IAV timescale in JJA is longer than 4 years, while that in DJF is shorter than 4 years. The IAV in DJF is much stronger than that in JJA. In both seasons, DIV has apparent peaks at decadal (around 10 years) and interdecadal (around 40-50 years) timescales, and a weak bidecadal signal (around 19 years). There is also a weak signal at CEV timescale in both seasons. The original SST anomaly and the corresponding time series of IAV, DIV and TRD are presented in Fig. 2 for JJA and Fig. 3 for DJF, respectively. There are two time series for IAV. One (shown by bars) is from directly wavelet coefficients, and the other (shown by a curve) is the difference between the SST anomaly and the sum of DIV and TRD. In both seasons, the magnitude of DIV is comparable to that of IAV. It is not clear how much of the large positive values in DIV may be due to the edge effect of wavelet. However, since we used the whole data length (127 years) for wavelet transform, the large positive value around 1960 should not be influenced by an edge effect at the DIV timescale. Thus, the large positive values of DIV in both seasons in 1990's may be reasonable. This DIV may be responsible for the frequently observed El Niño events in the 1990's.

3. SST ANOMALY PATTERNS

Figs. 4 and 5 present the linear regression patterns of SST anomaly with the three time series shown in Figs. 2 and 3, respectively. These patterns show how the SST anomaly in these seasons vary at IAV, DIV and TRD timescales in different oceanic areas. At the IAV timescale, both seasons show an El Niño-like SST anomaly distribution, with a positive global mean. In DJF, the positive anomaly in the eastern tropical Pacific and the negative anomalies in the extratropics in both hemispheres are stronger than those in JJA. At the DIV timescale, a positive center in the subtropical eastern Pacific off west coast of North America intensi-

fies. The SST anomaly in this area may have a great impact on the climate in the U.S. at the DIV timescale. Meanwhile, the North Atlantic basically varies with the same sign as the global mean SST anomaly at the DIV timescale. As the length of the timescale increases, the positive center in the tropics weakens, while the negative center in the extratropics in Northern Hemisphere intensifies. This implies that while the globe showing a warming trend, the extratropical North Pacific and the northern part of the North Atlantic show cooling trends with the largest cooling rate in the extratropical North Pacific.

4. RAINFALL ANOMALY PATTERNS

Preliminary results show that the areas suffered with floods and droughts may be linked to different timescales of the variability of the globally averaged SST anomaly (GMSST). In summers, a positive GMSST component at IAV timescale (Fig. 6a) may be related to severe droughts in the southeastern states while the floods in the south and west of the Great Lake, New England states, and the northwestern U.S. At the DIV timescale (Fig. 6b), a positive GMSST component may be related to a wetter eastern part of the U.S. while drier in the west. Severe flood may occur in the middle southern states of the U.S. Due to the global SST warming trend (Fig. 6c), the coastal states in the southeastern US become drier while most of the U.S., especially in the east coast of Canada and the Great Lake area become wetter. In winters, a positive GMSST at the IAV timescale (Fig. 6d) may be related to flood in east coast of the U.S. and California (especially its southern part), while drier in most other area, especially to the south of the Great Lakes and those in the northwestern states except for Pacific coastal area. At the DIV timescale (Fig. 6e), a positive GMSST may be related to the flood in Texas and California and drought in northwest states of the U.S. The global SST warming trend (Fig. 6f) tends to make most part of the U.S., especially the southern states wetter while northwest coastal states of the US drier.

The above patterns and the components of GMSST shown in Figs. 2 and 3 are used to estimate the impacts of the 1997-98 El Niño event on the anomalous seasonal rainfall distribution in the U.S. at different timescales. Fig. 6g shows the combined impact of 1997 SST anomaly at IAV, DIV and TRD timescales on the rainfall in the U.S. for the summer. Fig. 6h is the observed rainfall anomaly during 1997 summer. Various parts of the U.S. may be influenced differently depending on timescales. As seen from Fig. 2, all the three components in 1997 are positive. Thus, in most states along Atlantic coast is drier than normal, while the mid states and western coast area are wetter. Figs. 6i and 6j are the combined and observed rainfall patterns, respectively, for 1997/98 winter. The main features of the combined pattern are similar to those observed: the southeastern and western

coastal states are wetter, while northwestern states away from the west coastal area are drier.

The patterns shown in Fig. 6 are only the part of rainfall that may be related to the global scale (globally averaged) SST anomaly. Although Figs 4 and 5 have shown the corresponding SST anomaly patterns related to IAV, DIV and TRD components of GMSST, these may not reflect other SST anomaly influence on the rainfall in the U. S. due to SST anomaly distribution in space, which will be studied separately.

REFERENCES

- Chang, P., L. Ji, and H. Li, 1997: A decadal climate variation in the tropical Atlantic Ocean from thermodynamic air-sea interactions. *Nature*, **385**, 516-518.
- Folland, C. K., D. E. Parker, and F. E. Kates, 1984: Worldwide marine temperature fluctuations 1856-1981. *Nature*, **310**, 670-673.
- Latif, M. and T. P. Barnett, 1996: Decadal climate variability over the North Pacific and North America: dynamics and predictability. *J. Climate*, **9**, 2407-2423.
- Lau, K.-M. and H.-Y. Weng, 1998: Interannual, decadal-to-interdecadal and global warming signals in sea surface temperature during 1955-1997. *J. Climate*, in press.
- Zhang, Y., J. M. Wallace, and D. S. Battisti, 1997: ENSO-like interdecadal variability: 1900-1993. *J. Climate*, 1004-1020.

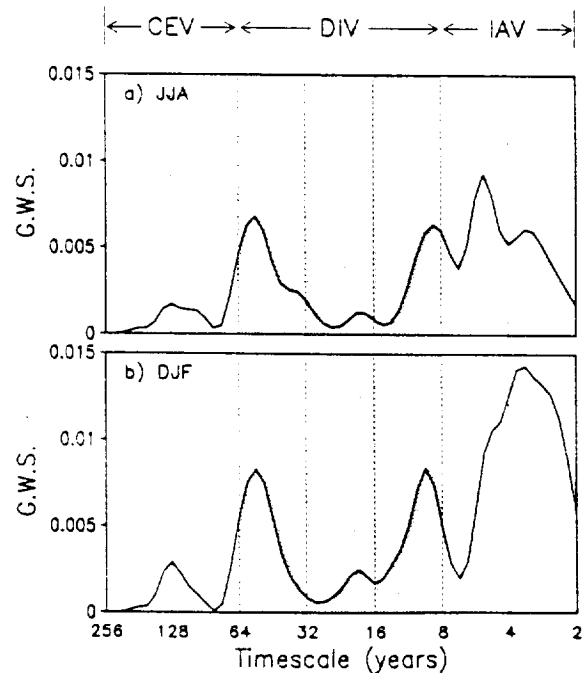


Figure 1: Global wavelet spectrum of the detrended SST anomaly for a) JJA and b) DJF

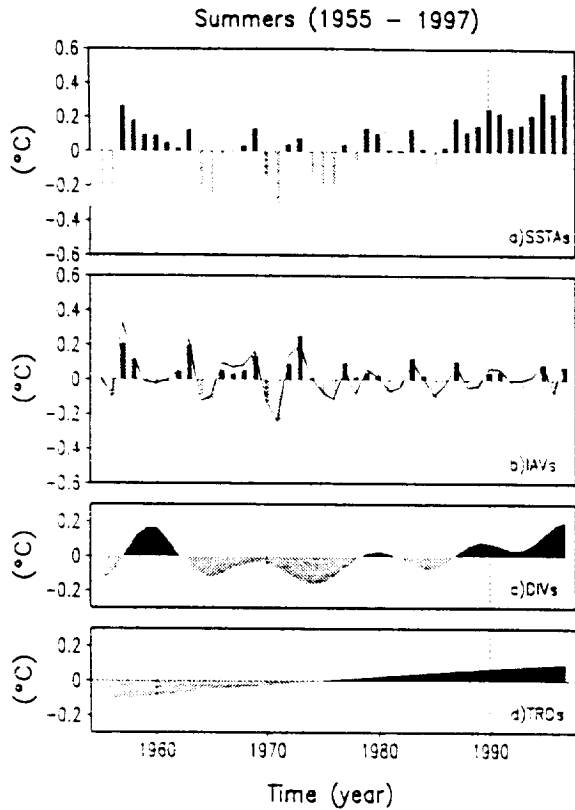


Figure 2: Global mean JJA's SST anomaly and its IAV, DIV and TRD components based on wavelet coefficients. The two IAV signals are explained in the text.

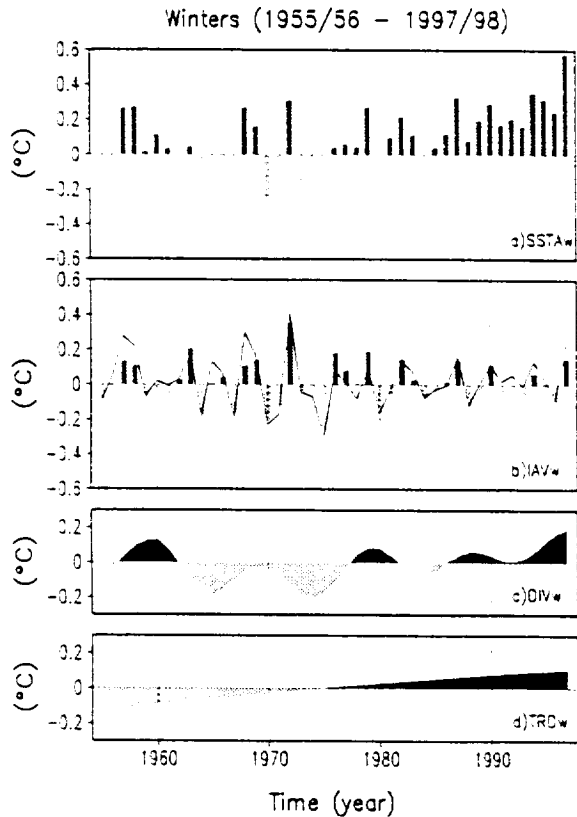


Figure 3: Same as Figure 2, except for DJF.

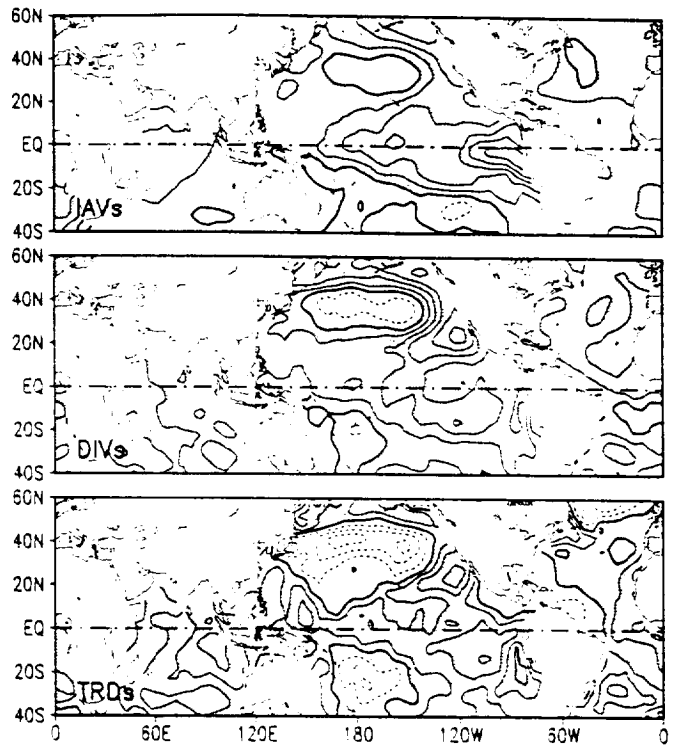


Figure 4: Linear regression of SST anomaly with global mean SST components for JJA.

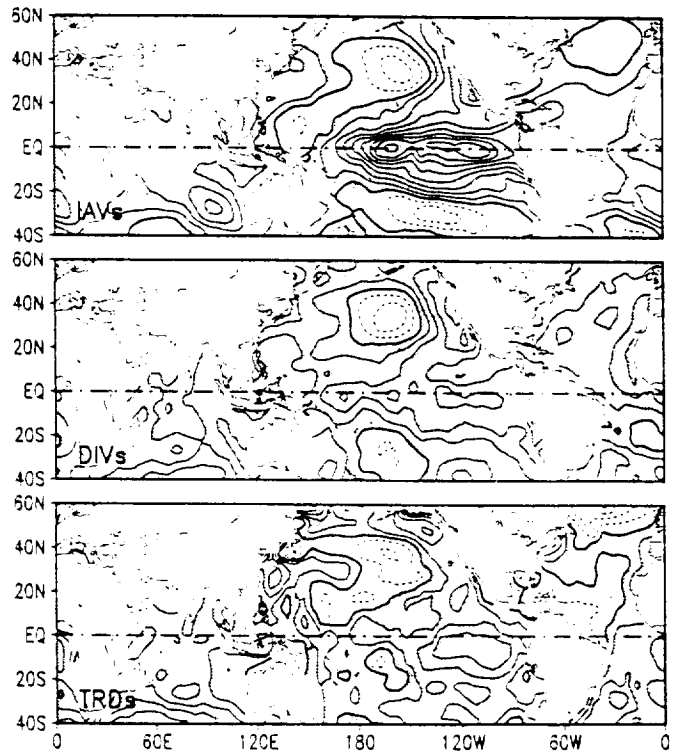


Figure 5: Same as Figure 4, except for DJF.

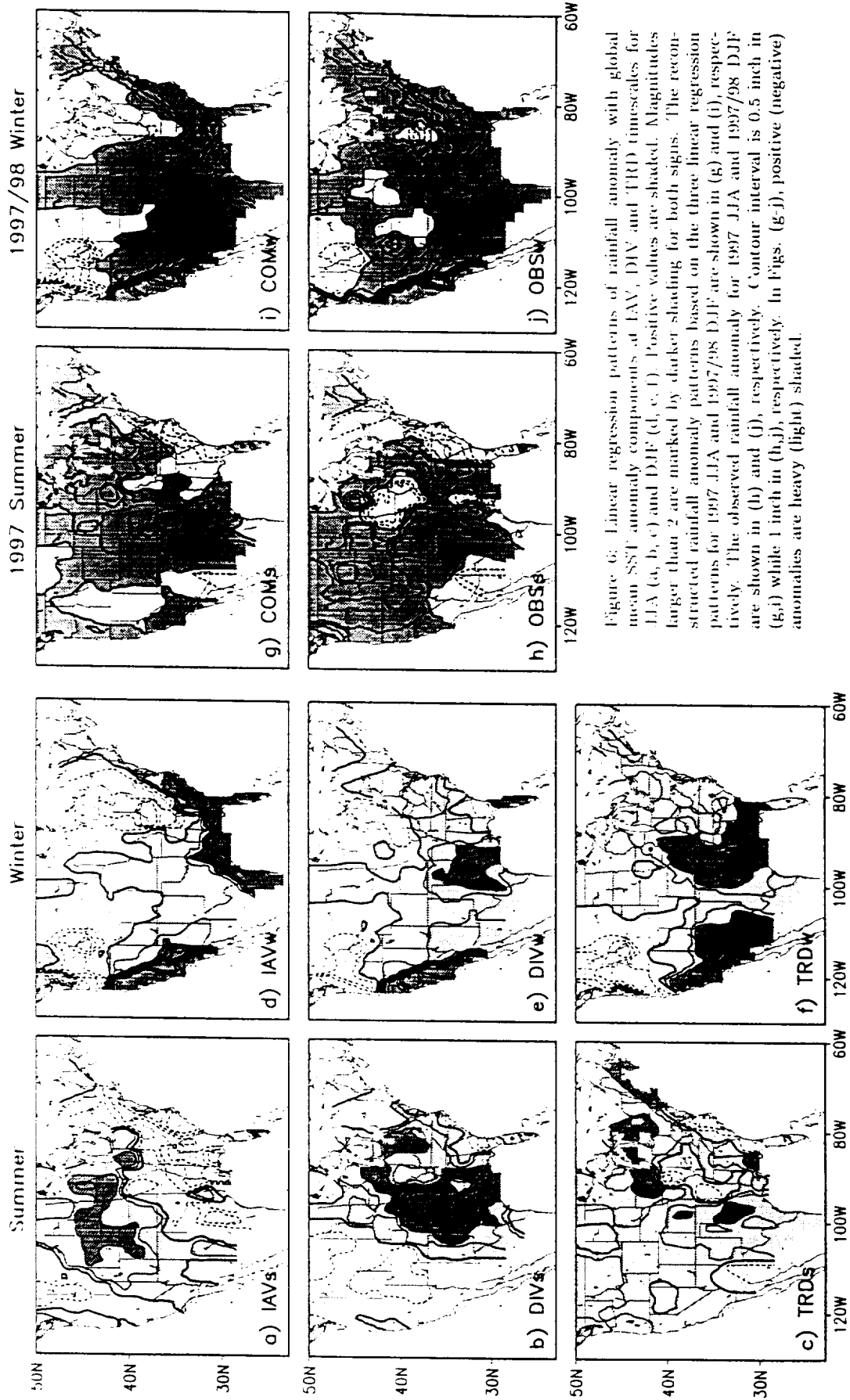


Figure 6: Linear regression patterns of rainfall anomaly with global mean SST anomaly components at IAV, DIV and TRD timescales for JJA (a, b, c) and DJF (d, e, f). Positive values are shaded. Magnitudes larger than 2 are marked by darker shading for both signs. The reconstructed rainfall anomaly patterns based on the three linear regression patterns for 1997 JJA and 1997/98 DJF are shown in (g) and (i), respectively. The observed rainfall anomaly for 1997 JJA and 1997/98 DJF are shown in (h) and (j), respectively. Contour interval is 0.5 inch in (g,i) while 1 inch in (h,j), respectively. In Figs. (g-j), positive (negative) anomalies are heavy (light) shaded.